Preparation and characterization of layered low-voltage ZnO varistors*

Wang Lihui(王立惠)[1], Gan Guoyou(甘国友)[1,†], Sun Jialin(孙加林)[2], and Yan Jikang(严继康)[1]

(1 Faculty of Materials and Metallurgical Engineering, Kunming University of Science and Technology, Kunming 650093, China)

(2 China Nonferrous Metal Mining (Group) Co., Ltd., Beijing 100055, China)

Abstract: Double-layered, low-voltage ZnO varistors have been fabricated by feeding two kinds of ZnO powders into a die using dry extrusion molding. Compared with ZnO varistors fabricated by the conventional route, the layered ZnO varistors have larger non-linear coefficients, lower breakdown electric fields, and lower leakage current densities. The improvement in electrical performance of the layered low-voltage ZnO varistors is attributed to the asymmetric band structure at grain boundary between the two layers.

Key words: layered ZnO varistor; non-linearity; electrical properties
DOI: 10.1088/1674-4926/30/3/033002 **PACC:** 6848；6630D；6170W

1. Introduction

Zinc oxide (ZnO) varistors with non-linear current–voltage ($I-V$) characteristics and energy-handling ability have been widely used for protecting electronic devices against voltage surges. With the development of microelectronics and large-scale integrated circuits, low-voltage ZnO varistors are now being used for surge protection in integrated circuits and in automobiles. These varistors have thus become an important topic in academic and industrial research[1–6].

The electrical characteristics of low-voltage ZnO varistors are closely related to their composition and microstructure, specifically the ZnO grain size and the structure at the grain boundaries[2,5]. Optimizing the process, the composition and thickness of conventional varistors were used as principal approaches for making low-voltage ZnO varistors[7–9]. However, the strength and energy absorption capability of the ZnO varistor decreases when its thickness is decreased[3]. Therefore, it is necessary to find a new method to fabricate high performance varistors without markedly reducing their thickness.

In this publication a novel structure for a double-layered, low-voltage ZnO varistor with improved electrical properties is described and a theory based on the potential barrier at the grain boundary between the layers is developed to explain the experimental results. These layered, low-voltage ZnO varistors were synthesized using two types of ZnO powders. One type of ZnO powder contained metal oxides additives, while the other type contained no dopants.

2. Experimental details

The compositions of two different types of ZnO mixed powders, A and B, are listed in Table 1. The structure of a double-layered, low-voltage ZnO varistor is shown in Fig. 1. Layers A and B are synthesized using compositions A and B, respectively. Composition A was prepared by ball milling a mixture of oxides with ZnO powder according to the mixing ratios given in Table 1. After being ball milled for 4 h by the conventional oxide mixing route, composition A was fed into a die together with composition B as shown in Fig. 1 and molded once. The powder was first heated in air from room temperature to 400 °C at a heating rate of 1 °C/min and kept at this temperature for 1 h to remove organic contaminants. Afterwards it was sintered at 1250 °C for 2.5 h in air, respectively. Finally, the prepared samples were slowly cooled down to room temperature.

The distribution of the elements in the samples were analysed by electron probe microanalysis (EPMA). The microstructure of the sintered samples was examined by scanning electron microscopy (SEM). The elements in the various phases were identified by energy dispersive X-ray spectroscopy (EDS).

The I–V characteristics of the samples were measured using a DC power supply, a micro amperometer and a voltmeter. The varistor voltages corresponding to 1 mA and 0.1 mA were measured to determining the threshold voltages. The leakage current $I_{\rm L}$ was determined at 0.75 $V_{\rm 1mA}$. In addition, the non-linearity coefficient α was determined by

Fig. 1. Structure of a double-layered low-voltage ZnO varistor.

* Project supported by the Science and Technology Commission of Yunnan Province (No. 2002GG09) and the Science Research Foundation of Kunming University of Science and Technology (No. 2007-15).

† Corresponding author. Email: ganguoyou@sina.com

Received 21 June 2008, revised manuscript received 11 December 2008

Table 1. Composition of layers A and B.

Layer	Composition (mol%)							
	ZnO	n-ZnO	TiO_2	La_2O_3	Cr_2O_3	Co_2O_3	MnO_2	SiO_2
A	82.5	15	0.5	0.5	0.5	0.5	0.25	0.25
B	100	–	–	–	–	–	–	–

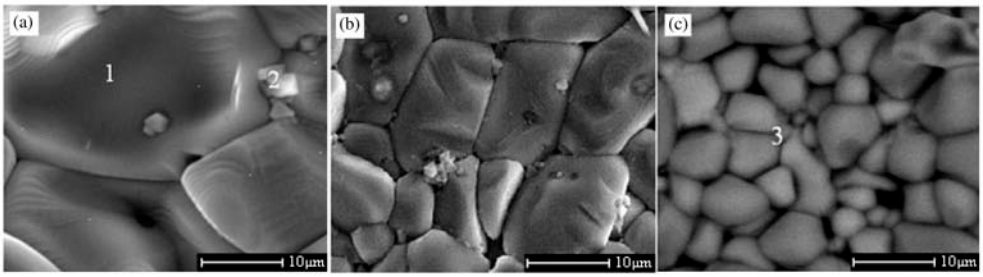

Fig. 2. SEM micrographs of (a) layer A, (b) the interface between layers A and B, and (c) layer B. All images were taken on a ZnO varistor sintered at 1250 °C.

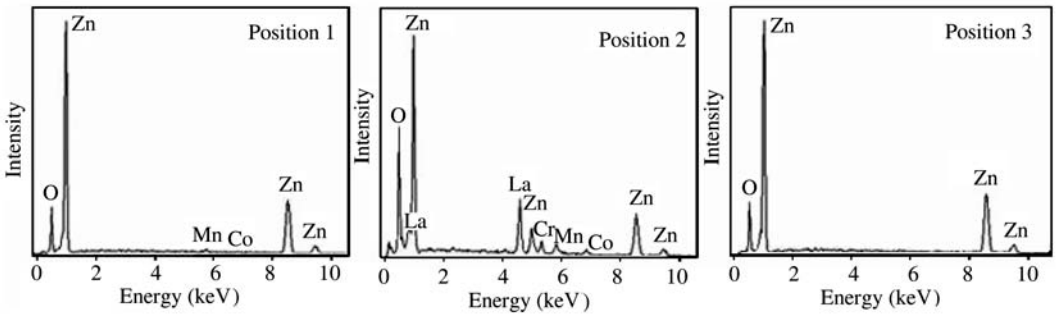

Fig. 3. EDS spectra for positions 1, 2 and 3 in Fig. 2.

$$\alpha = \frac{\lg I_2 - \lg I_1}{\lg V_2 - \lg V_1},$$

where $I_2 = 1.0$ mA, $I_1 = 0.1$ mA, and V_2 and V_1 are the voltages corresponding to I_2 and I_1, respectively.

3. Results and discussion

3.1. SEM and EPMA

The SEM images in Fig. 2 reveal the typical microstructure of the cross sections of the layered ZnO varistors sintered at 1250 °C. Displayed are the microstructures of layers A and B and their interface. From the SEM micrographs, it can be seen that the ZnO grain size in layer A is larger than that in layer B, which contains no additives. Similarly, at the interface the grain size in layer A is larger than in layer B.

The results of an EDS spot analysis at the locations indicated in Fig. 2 are presented in Fig. 3. From the EDS spectra and SEM pictures it can be concluded that a second phases containing increased amounts of La, Cr, Mn, and Co exists at the ZnO grain boundaries. In addition, the data indicates that Mn and Cr have diffused into the ZnO grains. In contrast, no intergranular phase was found in layer B.

The element distribution at the interface between layers A and B as observed using secondary electron imaging (EPMA-SEI) is shown in Fig. 4. The EPMA analysis revealed that the composition of layer A includes La, Mn, Cr, Ti, Si, and Co elements. No additives from layer A were found in layer B.

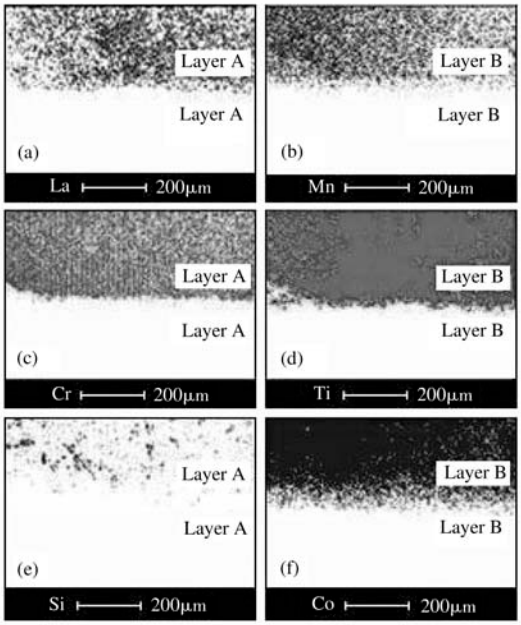

Fig. 4. EPMA-SEI images of layered low-voltage ZnO varistors sintered at 1250 °C showing the distribution of different dopend cations.

3.2. *I–V* characteristics

We used the optimized compositions for layer A, in which La is used as the key additive to obtain the non-linear *I–V* characteristic and the other elements are used to improve these non-linear characteristics[7]. Nano-ZnO plays a dominant role in accelerating ZnO grain growth during sintering

Table 2. Electrical properties of ZnO varistors.

Sample	Threshold voltage (V/mm)	Leakage current (μA)	Nonlinear coefficient
A	14.5	13	21
B	0.002	30	–
Layered structure	10	9	23

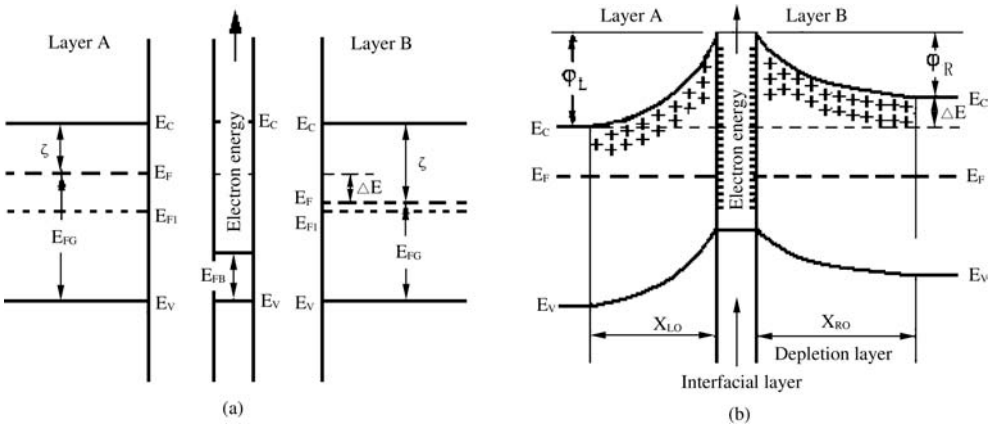

Fig. 5. Band diagram at the interface grain boundary: (a) Before contact; (b) In equilibrium after contact.

and enhances the mass transformation of the liquid phase as compared to the conventional route[10]. Furthermore, n-ZnO improves the macroelectrical property owing to its surface activity[10].

Table 2 compares the electrical properties of double-layered ZnO varistors with the respective properties of varistors based only on composition A or B. The samples based on either composition A or B were prepared by the conventional route. Double-layered samples were fabricated using compositions A and B according to the structure in Fig. 1. All the ZnO samples were sintered at 1250 °C.

According to Table 2, the behavior of sample B obeys Ohm's Law. No non-linearity was observed. Sample B exhibits the largest leakage current among the three sets of samples. Compared to sample B, sample A shows nonlinearity and has a lower voltage. The double-layered varistors has the highest non-linearity coefficient, while the leakage current and the voltage are lower as compared to sample A. Out of the analyzed set, the double-layered structure has the most advantageous electrical properties for a varistors.

3.3. Schottky barrier for the grain boundary between layers A and B

Double Schottky barriers are generated when majority carriers are trapped at interface states formed at grain boundaries[2]. When the concentration of additives in layer A is not equal to that in layer B, the difference in the Fermi levels gives rise to an electrical potential barrier across the ZnO grain boundaries at zero bias[11].

The position of the Fermi energy level within the bandgap can be determined by the thermal equilibrium electron and hole concentrations[11].

$$E_c - E_F = kT \ln \frac{N_c}{N_d},$$

where E_c is the energy at the conduction band edge, E_F is the Fermi energy, T is the absolute temperature, k is the Boltzmann constant, N_c is the effective density of states function of the conduction band, and N_d is the donor concentration.

In layer B, being the layer without dopants, the electrical properties of ZnO at room temperature is controlled by the intrinsic defects generated at high temperature[14]. The I–V characteristics across the grain boundary shows Ohmic behavior and no Schottky barriers are formed in ZnO bicrystals. Undoped ZnO exhibits n-type conductivity due to the lower formation energy of zinc interstitials and oxygen vacancies[12–14]. In contrast, in layer A the donor concentration of ZnO is even higher due to the doping by the additives. So, at the interface between layer A and layer B, the donor concentration changes. The value of the donor concentration is higher in layer A than in layer B, resulting in a larger Fermi energy in layer A. The difference in the Fermi levels gives rise to a variation of the electrical potential barrier height across the grain boundary. The band diagram of the grain boundary before contact is shown in Fig. 5(a) where E_{FG} and E_{FB} are the $E_F - E_V$ in the grain and grain boundary, respectively. After contact, as shown in Fig. 5(b), the potential barrier in equilibrium is higher on the left (in layer A) than on the right side (in layer B). Since the donor concentration in layer B is lower than in layer A, the depletion region is broader on the right side. The current density J_S, which is related to the voltage barrier and to temperature, follows the equation[15, 16]:

$$J_s = A^* T^2 \exp[(\beta E^{1/2} - \phi_B)/kT],$$

where A^* is the Richardson constant, ϕ_B is the interface potential barrier height, E is the electric field and β is a constant related to the potential barrier width by the relation:

$$\beta \propto 1/(r^* \omega)$$

where r^* is the number of grains per unit length and ω is the voltage barrier width.

Thus, if the temperature is constant, the current density was decreased with the increase in voltage barrier and the depletion width while the leakage current was generally shifted to lower values.

4. Conclusion

In the present study, the microstructure and the *I–V* characteristic of double-layered, low-voltage ZnO varistors were investigated. This work has shown that the layered ZnO varistor provides lower breakdown fields, lower leakage currents and higher non-linearity coefficients compared to varistors prepared by the conventional route. The improved current-voltage properties are attributed to a difference in the Fermi levels in the two layers which causes a variation in the electrical potential barrier height across the interface. This result suggests that the double-layered, low-voltage ZnO varistors can improve the macro-electrical properties while maintaining lower cost and a simple route.

References

[1] Gupta T K. Application of zinc oxide varistors. J Am Ceram Soc, 1990, 77(7):1817

[2] Levinson L M, Philips H R. Zinc oxide varistor—a review. Ceram Bull, 1986, 65(4):639

[3] Kazuo E. Degradation mechanism of nonohmic zinc oxide ceramics. Jpn J Appl Phys, 1980, 51(5): 2678

[4] Bowen L J, Avella F J. Microstructure, electrical properties and failure prediction in low clamping voltage zinc oxide varistors. J Appl Phys, 1983, 54 (5): 2764

[5] Clarke D R. Varistor ceramics. J Am Ceramic Soc, 1999, 82(3): 485

[6] Matsuoka M. Non-ohmic properties of zinc oxide ceramics. Jpn J Appl Phys, 1971, 10: 736

[7] Olsson E, Dunlop G L. The effect of Bi_2O_3 content on the microstructure and electrical properties of ZnO varistor materials. J Appl Phys, 1989, 66: 4317

[8] Sedky A, Abdeen M A. Nonlinear *I–V* characteristics in doped ZnO based-ceramic varistor. Physica B, 2007, 388: 266

[9] Hng H H, Knowles K M. Microstructure and current–voltage characteristics of multicomponent vanadium-doped zinc oxide varistors. J Am Ceram Soc, 2000, 83: 2455

[10] Shi J Z, Cao Q X, Wei Y G, et al. ZnO varistor manufactured by composite nano-additives. Mater Sci Eng B, 2003, 99: 344

[11] Neamen D A. Semiconductor physics and devices: basic principles. 3rd ed. New York: McGraw-Hill, 2003

[12] Hutson A R. Hall effect studies of doped zinc oxide single crystals. Phys Rev, 1957, 8: 222

[13] Hagemark K I, Chacka L C. Electrical transport properties of Zn doped ZnO. J Solid State Chem, 1975, 15: 261

[14] Ziegler E, Heinrich A. Electrical properties and non-stoichiometry in ZnO single crystals. Phys Status Solidi A, 1981, 66: 635

[15] Wang Y J, Wang J F, Li C P. Improved varistor nonlinearity via sintering and acceptor impurity doping. Eur Phys J AP, 2000, 11: 155

[16] Pianaro S A, Bueno P R, Longo E, et al. Electrical properties of the SnO_2-based varistor. J Mater Sci Mater Electron, 1998, 9: 159